

^(a)Permanent address: Department of Physics and Astronomy, University of Maryland, College Park, Md. 20742.

^(b)On leave from Centre d'Etudes Nucléaires de Fontenay-aux-Roses, B. P. No. 6, Fontenay-aux-Roses, France.

^(c)Consultant. Permanent address: Exxon Nuclear Company, Bellevue, Wash.

^(d)Consultant. Permanent address: Fusion Power Systems Division, Westinghouse Electric Company, Pittsburgh, Pa.

¹J. G. Cordey *et al.*, Nucl. Fusion **14**, 441 (1973).

²K. Bol *et al.*, in *Proceedings of the Fifth International Conference on Plasma Physics and Controlled Nuclear Fusion Research, Tokyo, Japan, 1974* (International Atomic Energy Agency, Vienna, Austria, 1975), Vol. 1, p. 77.

³L. A. Berry *et al.*, in *Proceedings of the Sixth International Conference on Plasma Physics and Controlled Nuclear Fusion Research, Berchtesgaden, West Ger-*

many, 1976 (International Atomic Energy Agency, Vienna, 1977), Vol. 1, p. 49.

⁴Équipe TFR, see Ref. 3; Vol. I, p. 69.

⁵J. W. M. Paul *et al.*, in *Proceedings of the Eighth European Conference on Controlled Fusion and Plasma Physics, Prague, Czechoslovakia, 1977*, Vol. II (to be published).

⁶V. S. Vlasenkov *et al.*, see Ref. 3, Vol. 1, p. 85.

⁷H. Eubank *et al.*, in *Proceedings of the Seventh International Conference on Plasma Physics and Controlled Nuclear Fusion Research, Innsbruck, Austria, 1978* (International Atomic Energy Agency, Vienna, Austria, 1979).

⁸J. Kim *et al.*, in *Proceedings of the Second Topical Meeting on Technology of Controlled Fusion, Richland, Washington, 1976* (National Technical Information Service, Springfield, Va., 1976), Vol. 4, p. 1213.

⁹K. Bol *et al.*, see Ref. 7.

¹⁰D. Post *et al.*, see Ref. 7.

¹¹P. E. Stott, Plasma Phys. **18**, 251 (1976).

Lower-Hybrid-Wave Heating in the Alcator-A Tokamak

J. J. Schuss, S. Fairfax, B. Kusse,^(a) R. R. Parker, M. Porkolab, D. Gwinn, I. Hutchinson, E. S. Marmor, D. Overskei, D. Pappas, L. S. Scaturro, and S. Wolfe
Francis Bitter Magnet Laboratory, Massachusetts Institute of Technology, Cambridge, Massachusetts 02139
(Received 13 April 1979)

We report the results of injecting 90 kW of microwave power near the lower hybrid frequency into the Alcator-A tokamak through a two-waveguide array. The observed plasma heating is in disagreement with that expected from linear waveguide-plasma coupling theory. From these results and auxiliary rf probe measurements we infer the non-linear formation of a high- k_{\parallel} wave power spectrum at the plasma edge.

There is currently extensive interest in raising plasma temperatures in tokamaks through auxiliary heating methods. Microwave heating of tokamaks near the lower hybrid frequency has been tried on ATC,¹⁻² Wega,³ Petaul,⁴ Doublet IIA,⁵ and recently on JFT2.⁶ In these experiments ion heating was obtained when the wave frequency was in the vicinity of the central lower-hybrid frequency, and some electron heating was also observed at lower densities. This ion heating was accompanied by a density rise and some impurity influx. No contradiction with the Brambilla waveguide-plasma coupling theory⁷ was reported in these experiments.

Here we report the results of injecting 90 kW of microwave power at 2.45 GHz into the Alcator-A tokamak through a split waveguide array. Ion heating occurs at well-defined values of central plasma density; below these densities electron

heating occurs. No density changes or impurity influx take place during the rf pulse. Contrary to previous experiments, the waveguide phasing has no effect on plasma heating. In addition, the densities at which heating occurs are significantly reduced from those expected from waveguide-plasma coupling theory.⁷ These results and the frequency spectra obtained from an rf probe suggest that the wave power spectrum formed near the plasma edge is shifted to higher $k_{\parallel} = \vec{k} \cdot \vec{B} / |\vec{B}|$ than predicted by linear theory.⁷

The waveguide array employed here consists of two adjacent independently driven waveguides mounted flush with the vacuum vessel walls; each has inner dimensions of 1.275 cm by 8.13 cm and are separated by a 0.09-cm-wide septum. Toroidally, the array is located 180° away from the limiter, which extends out 2.5 cm from the wall and defines a plasma minor radius of 10.0 cm

with a major radius of 54 cm. The vacuum windows in the waveguide were located outside the toroidal field magnets, so that the $\omega = \omega_{ce}$ layer was within the evacuated section of waveguide; nevertheless, no breakdown in the waveguide was observed at power densities up to 4.5 kW/cm², averaged over the waveguide mouth. With the exception of Petula,⁴ this power density is substantially higher than those reported in previous experiments. During this high-power operation over 85% of the incident power was coupled into the vacuum vessel by the array.

The linear theory of lower hybrid waves is well developed.⁸⁻¹⁰ Warm plasma theory predicts that $k_{\perp} = |\vec{k} \times \vec{B}|/|\vec{B}|$ will become large near the warm-plasma mode-conversion layer, at a density

$$\omega_{pi}^2 = \omega^2 / [1 - \omega^2 / (\omega_{ce} \omega_{ci}) + 2n_z (M_i a / m_e)^{1/2}], \quad (1)$$

where $n_z = k_{\parallel} c / \omega$, and $a = 3T_i / M_i c^2 + 0.75(\omega^2 / \omega_{ce} \omega_{ci})^2 T_e / M_i c^2$. When k_{\perp} is large, ion absorption of the lower hybrid wave can occur.¹¹ In addition, if $\omega / k_{\parallel} \sim 3v_{Te}$, the wave will be absorbed by electron Landau damping.¹² (This condition corresponds to $n_z = 5$ for $T_e = 1$ keV). Waves with $n_z < (1 - \omega^2 / \omega_{ce} \omega_{ci})^{-1/2}$ will mode convert into whistler modes; for a given n_z this occurs at a density which satisfies the relation

$$\frac{\omega_{pi}}{\omega} = \frac{n_z \omega}{(\omega_{ce} \omega_{ci})^{1/2}} - \left[n_z^2 \left(\frac{\omega^2}{\omega_{ce} \omega_{ci}} - 1 \right) + 1 \right]^{1/2}. \quad (2)$$

For $n_z = 1.5$, $B_T = 53$ kG (the value of B_T at the outside plasma edge when the central $B_{T0} = 62$ kG) and deuterium, this corresponds to $n_e = 7 \times 10^{13}$ cm⁻³, which occurs at $r > 9$ cm. Waves that mode convert into whistlers do not penetrate and do not heat the plasma center.

Waveguide-plasma coupling theory is also well developed.^{7,13} For the double waveguide employed here the theory predicts a wave power spectrum that monotonically decreases as n_z increases past 1 for oppositely phased waveguides ($\varphi = 180^\circ$); the part of the spectrum which penetrates to the plasma center is characterized by $n_z \sim 3$, which according to Eq. (1) would mode convert at $n_e = 3.8 \times 10^{14}$ cm⁻³ for $B_T = 62$ kG, $T_e = 1.0$ keV and $T_i = 0.8$ keV. Furthermore, only about 30% of the power spectrum has $n_z < 1.5$ and thus over 70% of the power penetrates at least past the plasma edge. When the waveguides are in phase ($\varphi = 0^\circ$) the power spectrum is compressed near $n_z = 1$ with over 80% of the wave power having $n_z < 1.5$ and being confined to the plasma exterior.

We, therefore, would have expected a marked reduction in central plasma heating when $\varphi = 0^\circ$ over $\varphi = 180^\circ$.

Figure 1(a) shows a typical plasma shot in the ion heating mode. The rf pulse produces no increase in density or loop voltage and no effect on the nitrogen, oxygen, carbon, or molybdenum impurity radiation; however, the fusion neutron flux increases by a factor of 15. Figure 1(b) shows the results of many such shots; enhanced neutron rates are observed at $\bar{n}_e \approx 1.6 \times 10^{14}$ cm⁻³ or central $n_{e0} \approx 2.4 \times 10^{14}$ cm⁻³. The peak neutron rate obtained was 2×10^{11} /sec. Sawteeth are clearly observable on the enhanced neutron rate, which indicates that its origin is within the $q = 1$ surface. During the rf pulse a high-energy tail appears on the charge-exchange-energy spectrum which is well correlated to the occurrence of neutron enhancement. Any change in bulk ion temperature as a result of wave heating is less than the 100 eV resolution of the charge-exchange diagnostics; only small changes in T_i are expected ($\Delta T_i < 150$ eV), as even for a 40% heating efficiency the available rf power is much less than the 270 kW total Ohmic-heating power and the 100 kW of Ohmic-heating power transferred from electrons to ions within $r = 5$ cm. It should be noted that the observed charge-exchange particles originate from ions superbanana trapped in the magnetic well formed by the pumping port gap in the toroidal magnet which rapidly ∇B drift out of the plasma. An up-down charge-exchange scan exhibits an asymmetry due to this drift and indicates that the energetic ion production is localized near the plasma center.

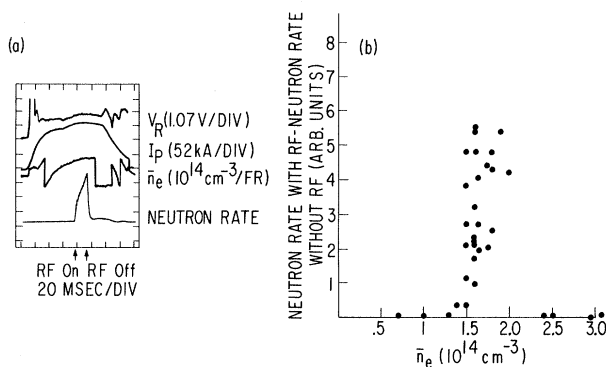


FIG. 1. (a) Typical plasma shot in ion heating mode: $B_{T0} = 62$ kG, $P_{rf} = 90$ kW, deuterium, and $\varphi = 180^\circ$; (b) neutron rates from several shots vs \bar{n}_e ; $B_{T0} = 62$ kG, $I_p = 150$ kA, $P_{rf} = 90$ kW, and $\varphi = 180^\circ$.

The experimental ion heating density bands for both D_2 and H_2 discharges are plotted in Fig. 2 for different values of B_T . The density at which ion heating occurred in hydrogen was ascertained from increases in the 8-keV charge-exchange flux, while in deuterium the neutron enhancement was used. The curves are theoretical predictions of the densities at which the mode-conversion layer will appear at the plasma center for typical Alcator-A parameters. The curve for $n_z=3$, which is the principal n_z expected theoretically, results in a higher density for heating than experimentally observed in deuterium. At $n_z=5$ the theoretical curve is in good agreement with the experimental points. A solution of the WKB wave equation¹¹ incorporating perpendicular ion Landau damping shows that for Alcator-A parameters and $n_z=5$ ion heating will occur at a density 10% below that of Fig. 2 in deuterium, which is in even better agreement with the experiment.

When the density is lowered below the ion heating density band, electron heating is observed. At $B_T=62$ kG and $1.0 \times 10^{14} \text{ cm}^{-3} < \bar{n}_e < 1.2 \times 10^{14} \text{ cm}^{-3}$ a 10% increase in central T_e is obtained from both electron cyclotron emission at $\omega=2\omega_{ce}$ and Thomson scattering measurements taken over consecutive identical shots; this increase in T_e would correspond to an rf heating efficiency greater than 35%. No energetic ion tail is measured by the charge-exchange diagnostics, indicating direct wave-electron heating. Electron Landau damping at $T_e=1100$ eV would require $\omega/k_{\parallel} v_{Te}=3$ or $n_z \sim 5$, which is far above that pre-

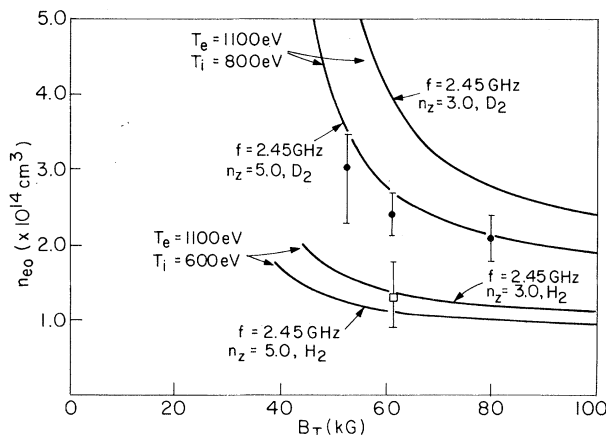


FIG. 2. Theoretically expected central densities at which mode conversion will occur for $n_z=3.0$ and $n_z=5.0$ in deuterium and hydrogen. Closed circles, experimental heating density in deuterium; open square, in hydrogen.

dicted by waveguide-plasma coupling theory, but consistent with the ion heating densities of Fig. 2. Thus, both the electron and ion heating can be explained by an upshift in the wave power spectra to $n_z \sim 5$.

The experimental results strongly suggest that this high- n_z spectrum originates near the plasma edge. The neutron flux is found to change by less than $\pm 10\%$ when the waveguide phase is varied from 0° to 180° over identical plasma shots.

From linear theory we would expect a factor-of-4 change in the power that can penetrate past the plasma edge when φ is varied from 0° to 180° . From this we postulate that the shift to higher n_z occurs at $r > 9$ cm, and thereby allows unchanged accessibility even as φ varies from 0° to 180° .

In Alcator-A this upshift in n_z from 3 to 5 would be more noticeable than in previous tokamak experiments. From Eq. (1) we can calculate the magnitude of the thermal correction to the lower hybrid density, $C = 2n_z(M_i a/m_e)^{1/2}/(1 - \omega^2/\omega_{ce}\omega_{ci})$, which for $n_z=3$ is about 0.5 for previous experiments,¹⁴ but 2.1 for Alcator-A. Thus due to the high $T_i \sim 800$ eV and $\omega^2 \approx \omega_{ce}\omega_{ci}$ of Alcator-A, an upshift in n_z from 3 to 5 would lower n_{LH} by 31%,

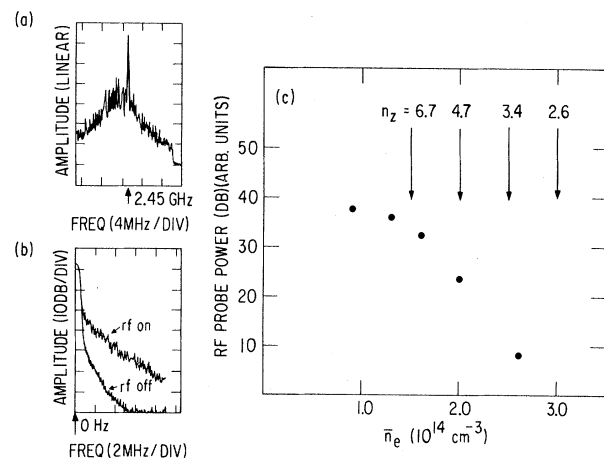


FIG. 3. (a) High-frequency spectrum of rf probe (linear scale). $B_T=62$ kG, deuterium plasma, $\bar{n}_e=2.8 \times 10^{14} \text{ cm}^{-3}$, $I_p=150$ kA, and $P_{rf}=80$ kW; the sudden drop in amplitude occurred at the end of the rf pulse. (b) Low-frequency spectrum of rf probe with and without rf power (10 dB/div). $B_T=62$ kG, deuterium plasma, $\bar{n}_e=1.6 \times 10^{14} \text{ cm}^{-3}$, $I_p=150$ kA, and $P_{rf}=80$ kW. (The peak at 0 Hz is a reference marker.) In (a) and (b) the spectrum analyzer bandwidth was 300 kHz. (c) Amplitude of high-frequency integrated probe signal vs \bar{n}_e for deuterium plasma, $I_p=150$ kA, $B_T=62$ kG, and $P_{rf}=75$ kW. The arrows indicate the values of n_z that will mode convert at the plasma center.

while in previous experiments n_{LH} could decrease only 18%.

Due to the high rf power densities present in Alcator-A, the parametric decay of the pump wave into lower-hybrid waves and ion-acoustic waves could occur at the plasma surface and cause an upshift in n_z . As previously shown, this decay process can significantly deplete the pump since the lower-hybrid decay wave then propagates along the pump-wave resonance cone.¹⁵ For our plasma-edge parameters ($n_e < 5 \times 10^{13}$ cm⁻³, $T_e < 10$ eV)¹⁶ and $T_e \gg T_i$ the inhomogeneous plasma convective threshold conditions can be satisfied for total waveguide powers of the order or less than 1 kW, which we easily exceed; the finite pump extent and homogeneous plasma threshold powers are even lower. It should be noted, that we have not measured the edge T_i ; if $T_i \sim T_e$ and the acoustic wave is strongly damped, the inhomogeneous plasma threshold power might be higher but still less than 75 kW.

Figure 3(a) shows the frequency spectrum obtained from the coaxial rf probe having a 1-mm-diam by 3-mm-long tip bent in the poloidal direction. This probe is located 90° toroidally away from the waveguides and 1.5 cm from the vacuum vessel wall in the limiter shadow; it can be shown that the ray originating from the waveguide mouth will not strike the probe due to the low density at the plasma edge (i.e., $n_e < 5 \times 10^{13}$ cm⁻³).¹⁵ The probe will, therefore, observe either surface waves or waves that cross the plasma column several times. The probe spectrum of Fig. 3(a) is asymmetrically downshifted and broadened in frequency. In addition, during the rf pulse a strong enhancement occurs in the amplitude of the low-frequency fluctuations, as shown in Fig. 3(b). [In the absence of rf, the low-frequency spectrum has a full width at half maximum (FWHM) of 150 kHz.] The reflected waveguide power spectrum also exhibits an asymmetrically frequency downshifted sideband of 2 to 4 MHz (FWHM), whose amplitude is 30 dB down from the pump. Similarly, frequency downshifted spectra are observed in the plasma interior by CO₂-laser scattering.¹⁶

Figure 3(c) shows the integrated intensity of probe signal versus \bar{n}_e . As the density rises, lower values of n_z are absorbed by the plasma column (as indicated by the arrows) and cannot reach the probe. The collected signal sharply drops as \bar{n}_e is raised above 1.5×10^{14} cm⁻³, which indicates that a major part of the power spectrum traversing the plasma has $n_z \sim 5$. Furthermore,

the low level of signal at high density suggests a small-amplitude surface wave. From this probe data, we infer that the pump wave may be significantly depleted while decaying into high- n_z lower hybrid waves near the plasma surface, which results in the anomalous heating obtained.

In conclusion, we have presented experimental plasma heating data and rf probe spectra from which we infer a nonlinear increase in n_z of the lower hybrid waves near the plasma surface. This n_z upshift could play an important role in future high-power rf heating experiments on toroidal plasma devices.

We are happy to acknowledge the diagnostic work carried out by D. Cope, M. Greenwald, Y. Takase, and J. West, and the engineering assistance of G. Chihoski and H. Israel. This work was supported by U. S. Department of Energy Contract No. ET-78-C-01-3019.

^(a)Permanent address: School of Applied and Engineering Physics, Cornell University, Ithaca, N. Y. 14853.

¹S. Bernabei *et al.*, in *Proceedings of the Third Symposium on Plasma Heating in Toroidal Devices, Varenna, Italy 1974*, edited by E. Sindoni (Editrice Compositori, Bologna, 1976), p. 68.

²M. Porkolab *et al.*, Phys. Rev. Lett. **38**, 230 (1977).

³C. Gormezano *et al.*, in *Proceedings of the Third Topical Conference on Radio Frequency Plasma Heating, California Institute of Technology, Pasadena, Cal., 1978* (to be published), Paper A3.

⁴P. Briand *et al.*, in *Proceedings of the Seventh International Conference on Plasma Physics and Controlled Nuclear Fusion Research, Innsbruck, Austria, 1978* (International Atomic Energy Agency, Vienna, Austria, 1979).

⁵J. L. Luxon *et al.*, Bull. Am. Phys. Soc., **23**, 821 (1978).

⁶T. Nagashima and N. Fujisawa, in *Proceedings of the Joint Varenna-Grenoble International Symposium on Heating in Toroidal Plasma, Grenoble, France, 3-7 July, 1978*, edited by T. Consoli and P. Caldirola (Pergamon, Elmsford, N. Y., 1979), Vol. II, p. 281.

⁷M. Brambilla, Nucl. Fusion **16**, 47 (1976).

⁸Thomas H. Stix, Phys. Rev. Lett. **15**, 878 (1965).

⁹Thomas H. Stix, *The Theory of Plasma Waves* (McGraw-Hill, New York, 1962).

¹⁰A. Bers, in *Proceedings of the Third Symposium on Plasma Heating in Toroidal Devices, Varenna, Italy 1974*, edited by E. Sindoni (Editrice Compositori, Bologna, 1976), p. 99.

¹¹M. Brambilla, Plasma Phys. **18**, 669 (1976).

¹²M. Brambilla, Nucl. Fusion **18**, 493 (1978).

¹³S. Bernabei *et al.*, Nucl. Fusion **17**, 929 (1977).

¹⁴C. M. Surko, R. E. Slusher, J. J. Schuss, R. R.

Parker, I. H. Hutchinson, D. Overskei, and L. S. Scaturro, to be published.

¹⁵K. L. Wong, P. Bellan, and M. Porkolab, *Phys. Rev. Lett.*, **40**, 554 (1978); K. L. Wong, J. R. Wilson, and

M. Porkolab, Princeton Plasma Physics Laboratory Report No. PPL-1499, 1979 (unpublished).

¹⁶L. S. Scaturro and B. Kusse, *Nucl. Fusion* **18**, 1717 (1978).

Electron-Density Structures in Laser-Produced Plasmas at High Irradiances

A. Raven

Rutherford Laboratory, Chilton, Didcot, Oxon, United Kingdom

and

O. Willi

Department of Engineering Science, Oxford University, Oxford, United Kingdom

(Received 26 March 1979)

Interferometric measurements have been made of the electron-density structures produced in plasmas generated by the interaction of 1.06- μm radiation with targets at irradiances I of 10^{16} W cm^{-2} . Strong profile steepening near critical density with an $I^{0.16}$ scaling is observed together with supercritical density bumps and structures attributable to magnetic field effects.

The effects of radiation pressure on the density profiles formed during the interaction of intense laser light with plasmas have been recently reported in the regime where the radiation pressure P_r is a fraction (0.2) of the plasma pressure P_c at critical density.¹ Three types of profile modification have been discussed theoretically² of which one type is consistent with numerical studies³ and favored by stability. In this Letter we present the results of an interferometric study at $\lambda = 266$ nm of the time evolution of density structures produced at irradiances of 10^{16} W cm^{-2} where $P_r > P_c$. Initial steepening of the profile with a step-height scaling of $\Delta n/n_c \propto I^{0.16 \pm 0.01}$ is observed followed by the development at later times of supercritical density structures. A model is proposed for these structures in terms of the plasma flow profiles. Structures are also observed that are attributable to the high magnetic-field pressure ($B^2/8\pi nkT \sim 0.5$) in the low-density corona.

The targets used consisted of small 40- μm -diam hollow glass microballoons or 1-mm-diam aluminum wires. The former were chosen to facilitate probing to high densities.¹ Irradiation of these targets was with a single 50-ps-full-width (at half maximum) pulse of between 0.5 and 2.5 J in a 15- μm focal spot giving irradiances on target of up to 10^{16} W cm^{-2} .

A portion of the main irradiating beam was split off and frequency quadrupled in two succes-

sive deuterated potassium dihydrogen phosphate crystals to generate a probe beam at 266 nm. The probe pulse of 150 μJ in 25 ps was used to illuminate the target from the side. Timing with respect to the main beam was to within 15 ps as measured by an EPL streak camera. An $f/2.5 \times 10$ ultraviolet microscope objective was used to image the target. Protection of the objective from target debris and scattered 1.06- μm light was achieved by the use of a 100- μm -thick quartz pellicle with a dielectric mirror coating on the front surface. The interferometer was of the Nomarski type⁴ and used a quartz Wollaston prism and a calcite Glan-Taylor prism mounted coaxially behind the microscope objective. Interferograms were recorded on Kodak HP5 film. Alignment and focusing were carried out in the He-Ne light with the interference fringes switched off and an empirically determined focal-length correction was then applied to focus the image in 266-nm light. A focal accuracy of 10 μm , which is necessary for the accurate analysis of the density profiles of the strongly refracting plasma,⁵ was achieved.

The interferograms were enlarged and fringe-position data were digitized with a computer-linked graphics tablet. Abel inversions⁶ were performed along lines normal to the main laser beam and the central values of such inversions, taken every 0.5 μm , were used to obtain the axial (Z) electron-density profiles.